Comparative analysis of neurogenesis in the myriapod *Glomeris marginata* (Diplopoda) suggests more similarities to chelicerates than to insects

Hilary Dove and Angelika Stollewerk*

Abteilung für Evolutionsgenetik, Institut für Genetik, Universität zu Köln, Weyertal 121, 50931 Köln, Germany
*Author for correspondence (e-mail: angelika.stollewerk@uni-koeln.de)

SUMMARY

Molecular data suggest that myriapods are a basal arthropod group and may even be the sister group of chelicerates. To find morphological indications for this relationship we have analysed neurogenesis in the myriapod *Glomeris marginata* (Diplopoda). We show here that groups of neural precursors, rather than single cells as in insects, invaginate from the ventral neuroectoderm in a manner similar to that in the spider: invaginating cell groups arise sequentially and at stereotyped positions in the ventral neuroectoderm of *Glomeris,* and all cells of the neurogenic region seem to enter the neural pathway.

Furthermore, we have identified an *achaete-scute*, a *Delta* and a *Notch* homologue in *Glomeris*. The genes are expressed in a pattern similar to the spider homologues and show more sequence similarity to the chelicerates than to the insects. We conclude that the myriapod pattern of neural precursor formation is compatible with the possibility of a chelicerate-myriapod sister group relationship.

Key words: Proneural genes, Neurogenic genes, Neurogenesis, Myriapod, *Glomeris marginata*

INTRODUCTION

Recent molecular and morphological data have challenged the traditional view that insects and myriapods are closely related (Hwang et al., 2001; Friedrich and Tautz, 1995; Boore et al., 1995; Akam et al., 1988; Patel et al., 1989a; Patel et al., 1989b; Abhzanov and Kaufman, 1999; Abhzanov and Kaufman, 2000; Damen et al., 2000; Abhzanov et al., 1999; Damen and Tautz, 1998; Damen et al., 1998; Telford and Thomas, 1998; Scholtz, 1990; Scholtz, 1992; Dohle and Scholtz, 1988; Harzsch and Dawirs, 1996; Whitington et al., 1991). This view was based on supposedly shared characters such as loss of second antennae, formation of Malpighian tubules, postantennal organs and trachea. However, a re-evaluation of these characters shows that they are prone to convergence (Friedrich and Tautz, 1995; Dohle, 2001). Instead, it is possible to find other characters that are strikingly similar between insects and higher crustaceans, but cannot be found in equivalent form in myriapods (Dohle, 2001). The characters in common in insects and crustaceans are the presence of neuroblasts, patterns of axonogenesis in early differentiating neurons, the fine structure of ommatidia and the expression patterns of segmentation genes (Dohle, 1997; Dohle, 2001). Some molecular data sets even suggest that the chelicerates and the myriapods are sister groups (Friedrich and Tautz, 1995; Hwang et al., 2001). However, morphological data supporting this hypothesis is still missing.

It has been shown recently that neurogenesis in the spider *Cupiennius salei* (chelicerate) shares several features with *Drosophila,* but that there are also several important differences. Similar to the generation of neuroblasts in *Drosophila*, invagination sites arise sequentially and at stereotyped positions in regions that are prefigured by proneural genes (Stollewerk et al., 2001), while neurogenic genes restrict the proportion of cells that adopt the neural fate at each wave of neural precursor formation (Stollewerk, 2002). However, in contrast to *Drosophila*, groups of cells, rather than single cells, adopt the neural fate at a given time. In addition, neural stem cells, comparable to *Drosophila* neuroblasts, could not be detected in the ventral neuroectoderm of the spider. Furthermore, there is no decision between epidermal and neural fate in the ventral neuroectoderm of the spider as in *Drosophila*; instead all cells of the neurogenic region enter the neural pathway.

In all four myriapod groups (Diplopoda, Chilopoda, Symphyla and Pauropoda), the general development of the ventral neuroectoderm follows the same pattern. Ventral to the limb buds, thickenings form as a result of cell proliferation. When the embryo begins to bend about a transverse fold in the middle of the trunk, these thickenings flatten (Anderson, 1973). After completion of ventral flexure, the middle part of the hemisegment sinks into the embryo forming a groove (Dohle, 1964). Cell proliferation takes place within this groove pushing newly formed cells towards the basal side and leading to the formation of stacks of cells that project out as rays from the edges of the groove. This structure is called the 'ventral organ'. During the course of neurogenesis the ventral organs are gradually incorporated into the embryo while epidermal cells overgrow the ventral nerve cord (Dohle, 1964). Neurogenesis has been analysed in a variety of representatives of all

myriapod groups, but failed to reveal stem cell-like neural precursors with morphological characteristics of insect or crustacean neuroblasts (Heymons, 1901; Tiegs, 1940; Tiegs, 1947; Dohle, 1964; Whitington et al., 1991). Furthermore, Whitington and co-workers (Whitington et al., 1991) showed that in the centipede *Ethmostigmus rubripes* the earliest central axon pathways do not arise from segmentally repeated neurons as in insects but by the posterior growth of axons originating from neurons located in the brain. In addition, the axonal projections and the cell body positions of the segmental neurons clearly diverge from the pattern described in insects and crustaceans (Whitington et al., 1991).

Here, we have analysed the pattern of early neurogenesis in the myriapod *Glomeris marginata* and compared it to the recently obtained data for the spider *Cupiennius salei* (Stollewerk et al., 2001; Stollewerk, 2002).

MATERIALS AND METHODS

Glomeris marginata

Adult *Glomeris marginata* (Myriapoda, Diplopoda) were collected in the city forest of Cologne, Germany, between April and August 2002. *Glomeris* were kept in 20×10 cm plastic containers at room temperature with high humidity provided by wet cloths and earth. The females made egg chambers out of earth to cover the eggs. The eggs were collected daily and kept separately until they were between 6- and 12-days old.

Archispirostreptus sp.

Adult *Archispirostreptus* were obtained from the Aquazoo in Düsseldorf, Germany. Ten adults were kept at 28°C in large terraria filled to a depth of at least 20 cm with earth. Females laid a clutch of eggs into the earth, approximately every 3 weeks, which were collected, staged, cleaned with bleach (under 5%) and frozen at –80°C for RNA extraction.

Dechorionization and fixation

Glomeris eggs were removed from their egg chambers by submerging them in water. They were transferred to a 2 ml Eppendorf tube and washed several times in water. They were then dechorionated by leaving them in bleach (under 5%) for 2 minutes and rinsing several times with water. Embryos were frozen at –80°C for RNA extraction or fixed in 1 ml heptane, 50 μl formaldehyde (37%) for later use. Embryos for antibody stainings were fixed for 20 minutes on a wheel and then washed several times with 100% ethanol and stored at –20°C. For in situ hybridizations, embryos were fixed for 4 hours on a wheel and washed with 100% methanol before storage at –20°C. After storage, at least overnight, the embryos could be devitelinized with tweezers for further staining.

PCR cloning

GmASH, *GmNotch*, *GmDelta, AsAsh,* and *AsDelta* were initially found by RT-PCR on cDNA synthesized from RNA extracted from 7- to 12-day *Glomeris*, or 2- to 3-week *Archispirostreptus* embryos, respectively. Degenerate primers for the respective genes were used as described by Stollewerk et al. (Stollewerk et al., 2001; Stollewerk, 2002). The obtained PCR fragments were cloned into the pZero vector (Stratagene) and sequenced. Larger fragments were obtained by rapid amplification of cDNA ends (Marathon cDNA Amplification Kit, Clonetech; GeneRacer Kit, Invitrogene). Sequence reactions were performed on plasmid preparations with BIG DYE and run on an Abi Prism automatic sequencer. The sequences obtained were deposited with GenBank (Accession Numbers: *GmDelta*, AJ36341; *GmNotch*, AJ36342; *AsDelta*, AJ36343; *AsNotch*, AJ36344; *AsAsh*, AJ36345; *GmAsh*, AJ36346; *TcASH*, AJ36347).

Sequence analysis

Sequences were analysed and aligned with related amino acid sequences taken from the NIH Blast database in Bioedit. Trees were constructed using the PAUP NJ minimum evolution algorithm with 1000 bootstrap replicates. Positions where an amino acid insertion was present in only one sequence were removed, as was the variable part of the loop for the Ash alignment. Since the portion of the Ash sequences that could be aligned is very short (the BHLH domain), the presence or absence of a loop was used as an extra character (32/57 informative characters). For Delta, the DSL domain and EGF repeats 1 and 2 were aligned (70/109 informative characters), for Notch the 5′ sequences up to EGF repeat 12 were aligned (266/311 informative characters).

In situ hybridization

Whole-mount in situ hybridizations were performed as described for *Danio rerio*, with the modification that 20× SSC pH 5.5 was used instead of 20× SSC pH 7.4, to reduce the background (Bierkamp and Campos-Ortega, 1993).

Histology and stainings

Phalloidin-rhodamine staining of *Glomeris* embryos was performed as has been described for flies (Stollewerk, 2000). Immunocytochemistry was performed as described previously (Stollewerk et al., 2001). The anti-phospho-histone 3 (PH3) antibody was provided by F. Sprenger (Institute for Genetics, Cologne). Histology was performed as described previously (Stollewerk et al., 1996).

RESULTS

The embryonic segments of *Glomeris marginata* arise sequentially. Shortly after formation of the germband [stage 1; stages after Dohle (Dohle, 1964)], the first five anterior segments that contribute to the head are visible: the antennal segment, the premandibular segment, the mandibular segment, the maxillar segment and the postmaxillar segment. Three leg segments can also be distinguished at this stage. The next leg segment forms from the posterior growth zone at stage 2, while owing to the formation of intersegmental furrows the remaining segments are more clearly visible (Dohle, 1964). At stage 3 limb buds arise on the antennal, the mandibular and the maxillar segments, as well as on the three leg segments. It is important to note that these anlagen are formed simultaneously. At the end of stage 3 limb buds are also visible on the fourth leg segment and a fifth segment has been generated by the posterior growth zone. A thickening of the cephalic lobe and the ventral neuroectoderm can be observed at stage 4. Limb buds are now also visible on the fifth and sixth segment. At stage 5 a ventral-dorsal furrow forms at the level of the postmaxillar segment, so that the embryo curves inward and the head eventually approaches the anal pads at stage 6.

Formation of invagination sites in the ventral neuroectoderm

To analyse the morphology of the ventral neuorectoderm in *Glomeris* we stained embryos at stage 4 with phalloidin-rhodamine, a dye that stains the actin filaments, and investigated the cell shapes in the confocal laser-scanning
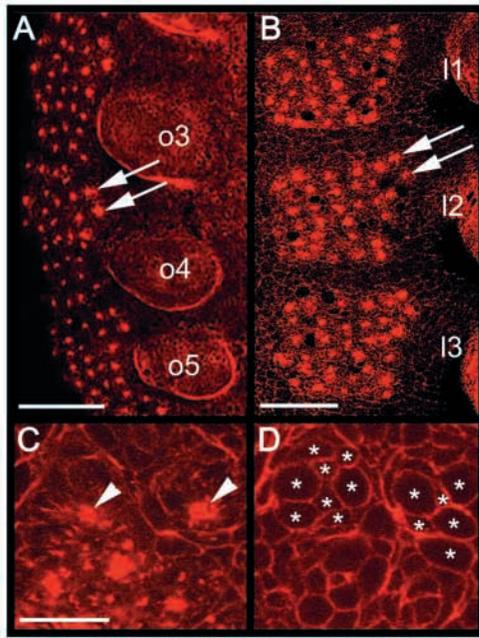
Fig. 1. (A-D) Comparison of the pattern of invagination sites in the myriapod *Glomeris marginata* and the spider *Cupiennius salei*. Confocal micrographs of flat preparations of embryos stained with phalloidin-rhodamine. Anterior is towards the top, the midline towards the left. (A) Pattern of invagination sites in the opisthosoma of the spider. The invagination sites are arranged in seven rows consisting of four to five invagination sites each. The arrows point to two lateral anterior invagination sites that can be easily identified in each hemisegment. (B) A strikingly similar pattern and number of invagination sites is visible in the leg segments of the myriapod. As in the spider, the invagination sites form seven rows consisting of four to five invagination sites each. The arrows point to two lateral anterior invagination sites. (C) Higher magnification of an apical optical section of invagination sites in the ventral neuroectoderm of *Glomeris*. The arrowheads point to two invagination sites. (D) Basal optical section of the same region shown in C. Basally enlarged cells are visible (asterisks) underneath the dots of high phalloidin-rhodamine staining. o3 to o5, opisthosomal segments 3 to 5; l1 to l3, leg segments 1 to 3. Scale bars: 100 μm in A; 50 μm in B; 10 μm in C,D.

microscope (LSM). At this stage a thickening of the neuroectoderm is already visible (see above) and the extension of the ventral neuroectoderm is clearly demarcated medially by the ventral midline and laterally by the limb buds. We made flat preparations of embryos stained with phalloidin-rhodamine and scanned them from apex to the base using the LSM. Similar to the situation in the spider, we detected dots of high phalloidin-rhodamine staining in apical optical sections of the neuroectoderm of the head segments and the first five leg segments (Fig. 1, see also Fig. 3). More basal optical sections of the same regions (at a depth of 11-21 μm from the apical surface of the embryo) revealed that groups of basally enlarged cells are located underneath the strongly stained dots, indicating that these dots mark the sites of invagination of neuroectodermal cells (Fig. 1).

As in the spider, 30-32 invaginating cell groups are arranged in a regular pattern of seven rows consisting of four to five invaginaton sites each. However, analysis of serial transverse sections revealed that up to 11 cells contribute to an individual invagination site (Fig. 2), while in the spider only five to nine cells were counted. Furthermore, in contrast to the spider, the ventral neuroectoderm has a multi-layered structure: the apical region covered by a single invagination site seems to be larger and the spacing between the individual invagination sites is narrower than in the spider (Fig. 1A,B). The reason for these morphological features is that the invaginating cell groups are located closer together and because of limited space come to lie over and above each other (Fig. 2B). The invaginating cells of a group do not all occupy a basal position as in the spider, but they also form stacks of cells (Fig. 2D). Since more cells contribute to an invagination site and the cell processes of the invaginating cells are not as constricted as in the spider, the apical region occupied by an individual invagination site is larger than in the spider (Fig. 2A).

A detailed analysis of different embryonic stages revealed that the invagination sites form sequentially in *G. marginata*. The same numbers of invaginating cell groups arise simultaneously in the five head segments and the first two leg segments, while the invagination sites are formed in an anterior to posterior gradient in the remaining segments. A tight comparison of the relevant embryonic stages showed that the
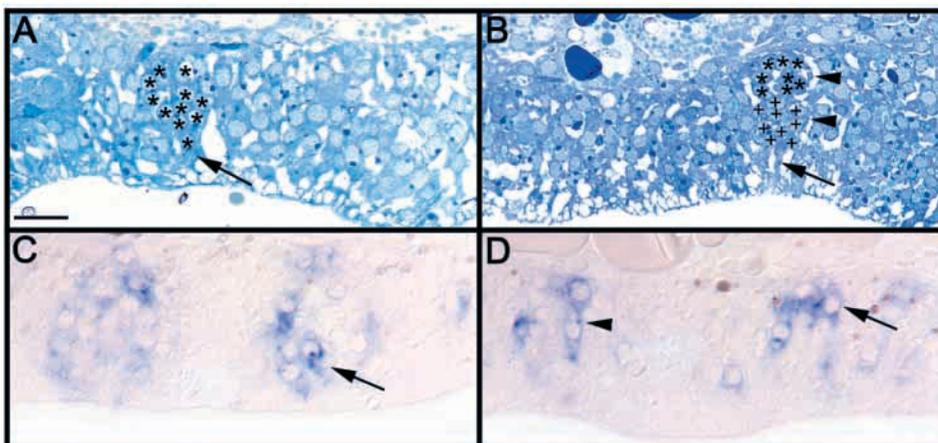

Fig. 2. (A-D) Apical-basal position of invagination sites in *Glomeris*. Transverse sections of untreated embryos (A,B) and embryos stained for a digoxigenin (DIG)-labelled *GmASH* probe (C,D). Basal is towards the top. (A) After formation of the first invagination sites, groups of up to 11 cells are visible on the basal side (asterisks) that are attached to the apical surface (arrow). (B) Groups of invaginating cells are located over and above each other (arrowheads) after formation of the third wave of neural precursors (asterisks and crosses). The cells are still attached to the apical surface (arrow). (C,D) *GmASH* is transiently expressed in the invaginating cell groups, which are located at different apical-basal positions (arrows). Some of the invaginating cell groups form stacks (arrowhead). Scale bar: 10 μm in A-D.

Fig. 3. (A-J) Sequential formation of invagination sites in the myriapod. Confocal micrographs of flat preparations of whole embryos (A-E) and the first two leg segments (F-J). Anterior is towards the top, the midline towards the left in F-J. (A,F) No invagination sites are visible at stage 1. (B,G) When the limb buds form at stage 2, the first invagination sites arise in the medial region of each hemisegment (arrowhead in G). (C,H) New invagination sites arise anterior, posterior and in-between the existing invagination sites (arrowheads in H) during the second wave of neural precursor formation. (D,I) At early stage 4, the next wave generates invagination sites that form a semicircle around the central region where invagination sites have already formed (arrowheads in I). (E,J) At stage

5, the embryo curves inwards and the ventral neuroectoderm stretches along the mediolateral axis. ant, antennal segment; l1 to l7, leg segments 1 to 7; md, mandibular segment; mx, maxillar segment; pmd, premandibular segment; pmx, premaxillar segment. Scale bars: 120 µm in A-E; 50 µm in F-J.
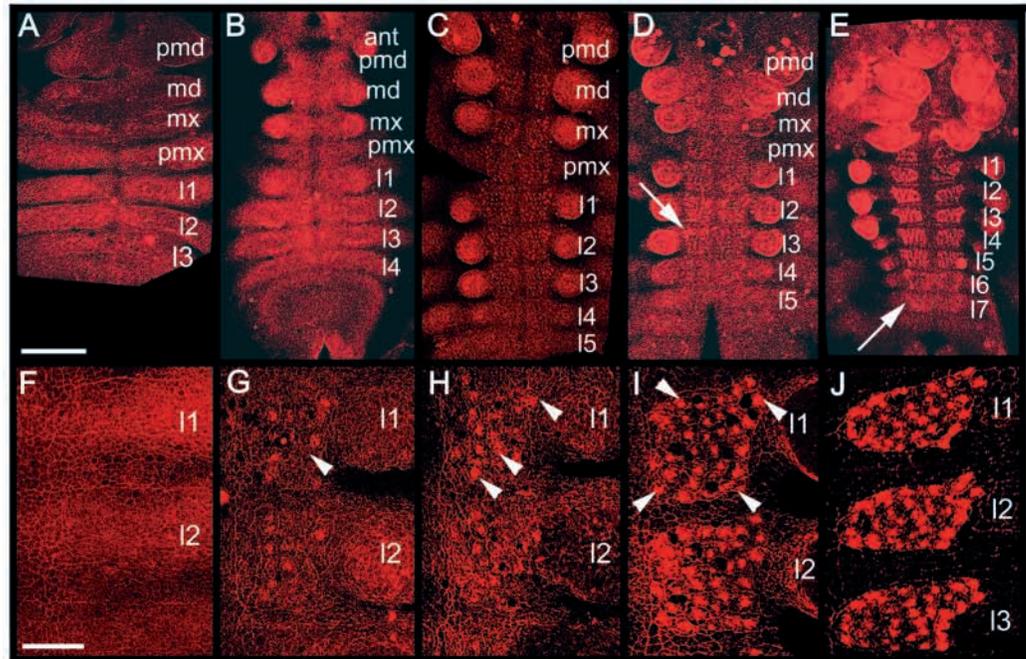
invagination sites are formed in four waves generating five to 13 invaginating cell groups each, as in the spider (Fig. 3, see also Fig. 7A-E). When the limb buds form, the first invagination sites arise in the medial region of each hemisegment in the five head segments and the first two leg segments at stage 2 (Fig. 3B,G). During the second wave of invagination site formation at stage 3, new invaginating cell groups arise anteriorly, posteriorly and in-between the existing invagination sites (Fig. 3C,H). The next invagination sites to arise form a semicircle around the central region where invagination sites have already formed (Fig. 3D,I). During the last wave of generation of invagination sites, invaginating cell groups arise in an anterior medial region and in between the existing invagination sites (compare also Fig. 7E). Although the embryo then curves inward and the ventral neuroectoderm stretches along the mediolateral axis, the arrangement in seven rows is maintained (Fig. 3E,J).

In summary, the data show that, as in the spider, groups of invaginating cells are generated in four waves that show a regular pattern strikingly similar to the arrangement of invagination sites in the spider.

Proliferating cells are associated with invagination sites

The thickening of the ventral neuroectoderm is a result of cell proliferation (Anderson, 1973). To see whether there is a connection between cell proliferation and formation of invagination sites, we double stained embryos with the mitotic marker anti-phospho-histone 3, to analyse the pattern of cell divisions, and phalloidin-rhodamine, to visualize the invagination sites.

In contrast to the spider, in which cell proliferation does not coincide with the formation of invagination sites (Stollewerk

et al., 2001), in *Glomeris* mitotic cells are associated with invagination sites and seem to prefigure the regions where invagination sites arise in the ventral neuroectoderm (Fig. 4). During formation of the first invagination sites at least one mitotic cell abuts the invaginating cell group (Fig. 4D-F), while groups of cells and individual cells could be detected in the regions where invagination sites form hours later (Fig. 4A-C). Most cell divisions occur in the apical cell layer (data not shown), as in the spider. It was not possible from these experiments to determine whether the cells of a particular invagination group are clonally related.

Isolation of proneural and neurogenic genes

The sequential formation and the regular pattern of the invagination sites in the ventral neuroectoderm of *Glomeris* suggest that, as in *Drosophila* and the spider *Cupiennius salei*, proneural and neurogenic genes regulate the recruitment of neural precursor cells from the neurogenic region. It has been shown recently in the spider that the proneural gene *CsASH1* is expressed before formation of the invagination sites in the appropriate regions of the ventral neuroectoderm (Stollewerk et al., 2001). Functional analysis revealed that the gene is responsible for the establishment of the neural precursors. Furthermore, one *Notch* and two *Delta* homologues of the *Drosophila* neurogenic genes restrict the proportion of cells that are recruited for the neural fate at each wave of neural precursor formation. To see whether a similar genetic network is involved in early neurogenesis in *Glomeris* we have cloned *achaete-scute*, *Notch* and *Delta* homologues. We also cloned homologues from *Archispirostreptus sp.*, a distantly related millipede, to ensure that the data collected from *Glomeris* is representative of Diplopod millipedes. Conserved features found in *Notch*, *Delta* and *acheate-scute* homologues allowed

Fig. 4. (A-F) Proliferating cells are associated with invagination sites. Confocal micrographs of flat preparations of embryos stained with phalloidin-rhodamine (red) and anti-phospho-histone 3 antibodies (green). Anterior is towards the top and the midline towards the left in D-F. (A-C) Single mitotic cells are associated with invagination sites that have already formed. The arrow in A points to an invagination site. The arrow in B points to a mitotic cell located at the same position as the invagination site indicated in A. The overlay of A and B is shown in C. (D-F) During formation of the first invagination sites in the central region of the hemisegment (arrowheads and arrow in D), mitotic cells are located at the centre of the invagination sites (arrowheads in E and F) or close to the invagination site (arrows in E and F). l1 to l2, leg segments 1 to 2. Scale bars: 50 µm in A-C; 10 µm in D-F.
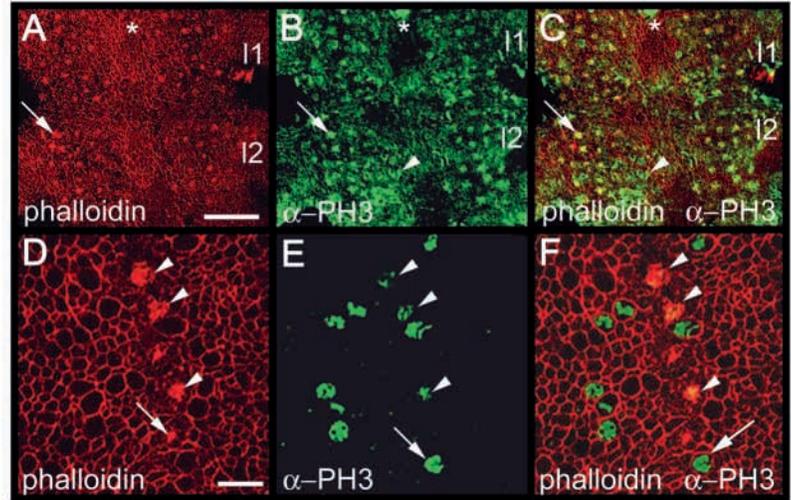
us to amplify small fragments of these genes from *Glomeris* and *Archispirostreptus sp.* cDNA. Only one fragment per species was found for each gene.

Rapid amplification of the 5′and 3′ ends (RACE) of *GmASH* resulted in a 1000 bp fragment with an 804 bp open reading frame (ORF), *Archispirostreptus* 5′ and 3′ RACE led to a 1200 bp fragment with an ORF of 864 bp. Both sequences have a single start codon with a short conserved motif also found in the *CsASH* genes, as well as upstream and downstream stop codons. The deduced amino acids of full-length *GmASH* and *AsASH* sequences showed a similarity of 61%, with 86% identical amino acids in the bHLH domains. The deduced amino acid sequence of *GmASH* is 83% identitical to *Homo sapiens* Achaete-Scute Complex homolog-like 1, while the *Archispirostreptus* sequence is 81% identical to the *Gallus gallus* transcriptional regulator CASH over the region of the bHLH domain. Outside of this domain, it is only possible to align a short conserved domain at the end of the protein. The alignment of the bHLH domains with other ASH proteins showed that, in contrast to insects, the millipede sequences, like their spider and vertebrate homologues, have a highly reduced loop (Fig. 5A). A tree was constructed from an alignment of the bHLH domains of nine insect, five vertebrate, two *Cupiennius salei* and the myriapod sequences (Fig. 6A). The node joining the myriapod, spider and vertebrate sequences has very high bootstrap support (94), while that joining the insects has low support.

Larger fragments of the *GmDelta* and *GmNotch* genes were amplified by 5′ RACE. This resulted in a 850 bp *GmDelta* sequence with an open reading frame of 280 amino acids covering a part of the N-terminal signal sequence, the DSL domain and EGF repeats 1 and 2, and a 1110 bp *GmNotch* sequence with a 377 deduced amino acid sequence comprising the N terminus and the first 12 EGF repeats. For both sequences, it was not possible to unambiguously identify the start codon.

For Delta, an *Archispirostreptus* sequence covering the DSL domain and EGF repeats 1 and 2 with 81% similarity to the *Cs*Delta1 protein was isolated. The complete *Gm*Delta sequence shares 57% identical amino acids with *Cs*Delta1, while the fragment similar to *As*Delta has a similarity of only
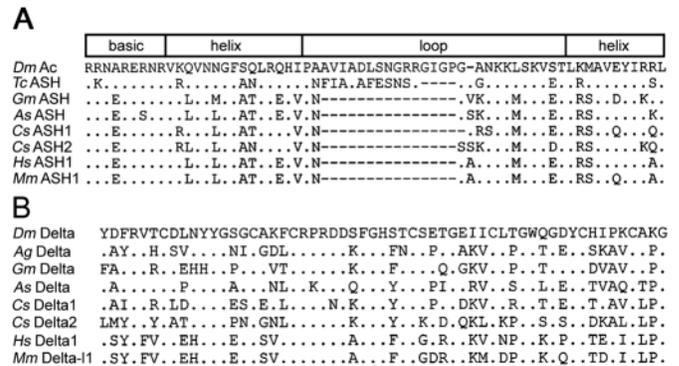

Fig. 5. (A,B) Comparison of the deduced amino acid sequences of the conserved domains of *GmASH* and *GmDelta*, and their relationships to the same protein regions of other species. (A) The alignment compares the basic domain, the two helices and the loop region of *GmASH* with the bHLH region of another diplopod, two insects, two vertebrates and two spider sequences. Note that the loop region of *Glomeris* ASH is reduced to the same extent as in the spider and vertebrate bHLH domains. The *GmASH* bHLH domain shows the highest similarity to the same region of the millipede *Archispirostreptus* sp. See text for further details. (B) The alignment compares the highly conserved DSL domain (Delta, Serrate, Lag2) of GmDelta with the DSL domains of the same species used for the alignment in A. The *Gm*Delta DSL domain shows the highest similarity to the same protein region of *Anopheles gambiae* (67% identical amino acids), *Archispirostreptus* sp. and *Cupiennius salei* Delta1 (65% identical amino acids each). *Ag*, *Anopheles gambiae*; *As*, *Archispirostreptus* sp.; *Cs*, *Cupiennius salei*; *Gm*, *Glomeris marginata*; *Hs*, *Homo sapiens*; *Mm*, *Mus musculus*.

62% with *Cs*Delta1. An alignment of the DSL domain shows that these sequences are highly conserved (Fig. 5B). The DSL domain and EGF repeats 1 and 2 from two insect species, five vertebrates, the two myriapods, the spider *Cupiennius salei* and one ascidian sequence (*Ciona savigny*) were aligned to create the tree shown in Fig. 6B. Here, the insects and the vertebrates form two clear groups, while the myriapods and the spider form another. All three of these groups have relatively high
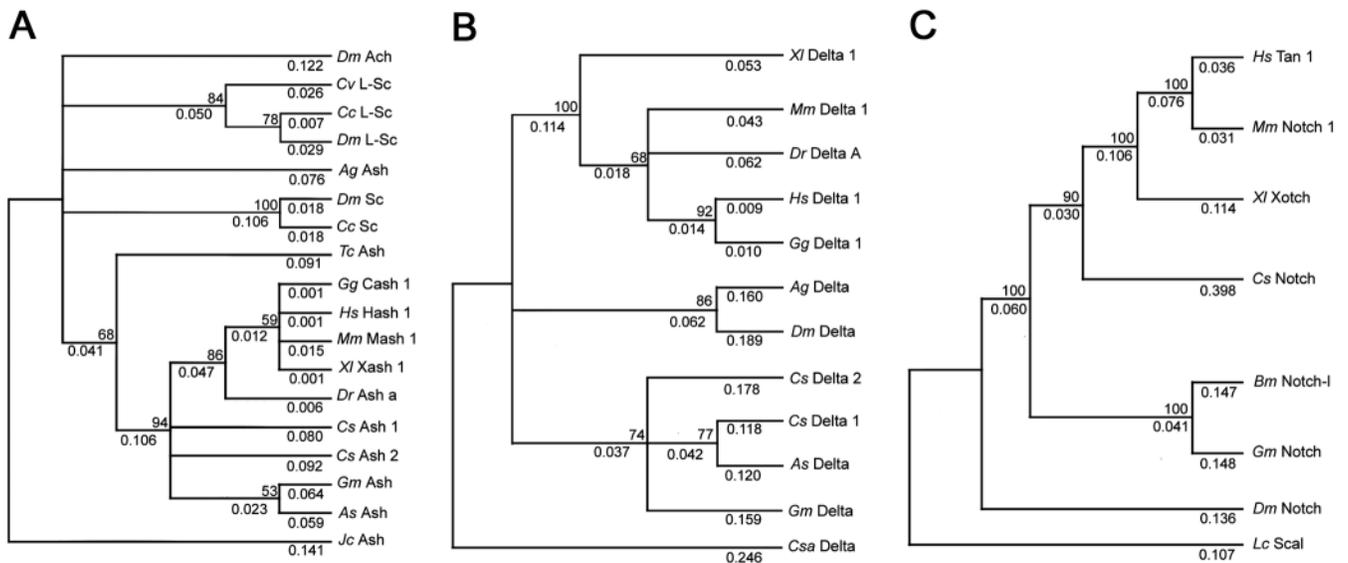
Fig. 6. (A-C) Phylogeny of the conserved domains of the *achaete-scute*, *Delta* and *Notch* homologues. The trees were constructed using the neighbour-joining algorithm (see Materials and Methods for further details). The numbers at the nodes are the bootstrap values given in percent (1000 replicates). Nodes without numbers have bootstrap values below 50%. The numbers below the branches are the branch lengths. (A) The tree was constructed from an alignment of the bHLH domains of nine insect, five vertebrate, two spider and two myriapod sequences. Both myriapod homologues group outside the insect genes together with the spider and vertebrate homologues. (B) The tree was created from an alignment of the DSL domains and the adjacent highly conserved EGF-repeats 1 and 2 from two insect species, five vertebrate, two myriapod, an ascidian and the two spider sequences. The insects and the vertebrates form two clear groups, while the myriapods group with the spider sequences. (C) The tree was constructed from an alignment of the obtained GmNotch sequence (5′ region up to EGF-repeat 12) with the same region of four vertebrate and three invertebrate Notch homologues. The myriapod sequence groups with the chelicerate *Boophilus microplus*, while the spider homologue forms a group with the vertebrates. The node joining the chelicerates with the vertebrates and the myriapod has a high bootstrap support (100%). Genes: *L-sc*, *lethal of scute*; *Sc*, *scute*; *Ac*, *achaete*; *Ash*, *achaete-scute homologue*; *Scal*, *scalloped wings*. Species: *Ag*, *Anopheles gambiae*; *As*, *Archispirostreptus* sp.; *Bm*, *Boophilus microplus*; *Cc*, *Ceratitis capitata*; *Cs*, *Cupiennius salei*; *Csa*, *Ciona savigny*; *Cv*, *Calliphora vicina*; *Dm*, *Drosophila melanogaster*; *Dr*, *Danio rerio*; *Gg*, *Gallus gallus*; *Gm*, *Glomeris marginata*; *Hs*, *Homo sapiens*; *Jc*, *Junonia coenia*; *Lc*, *Lucilia cuprina*; *Mm*, *Mus musculus*; *Tc*, *Tribolium castaneum*; *Xl*, *Xenopus laevis*.

bootstrap support: insects, 86%; vertebrates, 100%; spider and myriapods, 74%.

The obtained *Glomeris* Notch sequence, which shares 68% of its amino acids with the *Boophilus microplus* (chelicerate) Notch homologue, was aligned with seven Notch homologues to create the tree shown in Fig. 6C. The high sequence similarities between the *Glomeris* and the *Boophilus* proteins are reflected by the tree, where the node joining the Chelicerates with the vertebrates and *Glomeris* has a bootstrap support of 100% (Fig. 6C). The insect sequences, in contrast, are joined by a node with less than 50% support.

Expression pattern of *GmASH* during neurogenesis

GmASH transcripts were first detected before formation of the limb buds at stage 1. At this time no invagination sites are visible in the ventral neuroectoderm (Fig. 7A). The gene is expressed in neuroectodermal cells in the middle of each hemisegment in the head and the first two leg segments at heterogeneous levels (Fig. 7F). Groups of cells express high levels of the gene, while there is a weak uniform expression in the remaining regions (Fig. 7F). At stage 2 invagination sites arise in the expression domains of *GmASH* (Fig. 7B). At this time transcripts can be detected anterior, posterior and in between the first invagination sites (Fig. 7G, Fig. 8A). Again the next invagination sites to arise are generated in the regions

of *GmASH* expression (Fig. 7C). Although the gene is simultaneously expressed in the head segments and the first two leg segments, the expression domains in the antennal, premandibular, mandibular and maxillar segments seem to be smaller than in the remaining segments (Fig. 8A-D). At stage 3 the expression domains of *GmASH* form a semicircle around the area where invagination sites have already formed (Fig. 7H, Fig. 8B). This expression pattern again prefigures the regions where invagination sites will be formed hours later (Fig. 7D). Before the last wave of formation, *GmASH* is expressed in the corresponding regions in between and anterior-medial to the existing invagination sites. In addition, the gene is transiently expressed in the invaginating cell groups and in the neural precursors of the peripheral nervous system (Fig. 7J, Fig. 8C,D).

In summary, the data show that the *Glomeris achaete-scute* homologue is expressed prior to invagination of the neural precursors in the appropriate regions, similar to the spider gene.

Expression patterns of *GmDelta* and *GmNotch*

GmDelta is first expressed during the first wave of neural precursor formation at stage 2. Transcripts can be detected at low levels in all ventral neuroectodermal cells, but accumulate at higher levels in the invaginating cell groups, similar to the
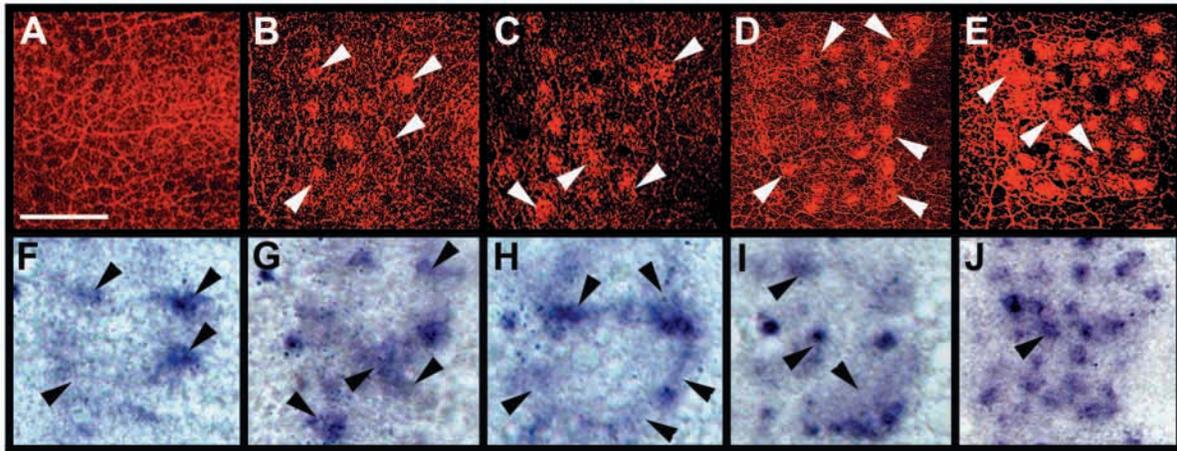
Fig. 7. (A-J) *GmASH* prefigures the regions where invagination sites arise. Confocal micrographs (A-E) and light micrographs of (F-J) of the first leg hemisegment. Anterior is towards the top, the midline is towards the left. (A,F) *GmASH* is expressed at heterogeneous levels in the central region of the hemisegment before formation of the invagination sites at stage 1 (arrowheads). (B,G) The first invagination sites (arrowheads in B) arise in the expression domains of *GmASH* at stage 2. At this time the gene is expressed in distinct regions of the hemisegment (arrowheads in G). In addition, *GmASH* shows transient expression in the invaginating cells. (C,H) At stage 3, the second wave generates invagination sites in the regions prefigured by *GmASH* (arrowheads in C, compare to G). At this time, the expression domains of *GmASH* form a semicircle around the central region where an invagination site have already formed (arrowheads in H). (D,I) Again invagination sites arise in the expression domains of *GmASH* (arrowheads). At this time the gene is re-expressed in distinct regions (arrowheads in I). (E,J). In these regions the last invagination sites arise during the fourth wave of neural precursor formation at late stage 4. *GmASH* expression is transiently maintained in the invaginating cell groups (arrowhead in J). Scale bar: 50 µm in A-J.

expression pattern of the spider *CsDelta2* gene. *GmDelta* is also expressed in all invagination sites generated subsequently (Fig. 9D-F). The expression seems to be rapidly down regulated, since transcripts cannot be detected in all invagination sites generated during different waves (Fig. 9A,B,D,F).

GmNotch is expressed in segmentally repeated stripes at stage 1, but shows a stronger expression in the ventral neuroectoderm. During formation of the first invagination sites the expression in stripes becomes restricted to the dorsal part

of the embryo, lateral to the limb buds (Fig. 10D). *GmNotch* is expressed at weak levels in almost all cells of the ventral neuroectoderm up to leg segment 3 (Fig. 10D). During the next wave of neural precursor formation at stage 3, there is a clear heterogeneity in the expression levels of *GmNotch* (Fig. 10A). This expression pattern is maintained during subsequent waves of neural precursor formation. *GmNotch* expression extends to more posterior segments during the course of neurogenesis. As in the anterior segments, the expression is uniform during the first wave of neural precursor formation and shows

Fig. 8. (A-D) Expression pattern of *GmASH*. Flat preparations of whole embryos stained for a DIG-labelled *GmASH* probe. Anterior is towards the top. (A) An anterior to posterior gradient of *GmASH* expression is visible in the neurogenic regions of the embryo. The mediolateral extension of the *GmASH* expression domain is smaller in the head segments. An identical *GmASH* expression pattern is visible in the leg segments 1 and 2 (arrow), while the former expression pattern of anterior segments can be detected in leg segment 3 (arrow; compare to Fig. 7F,G). (B) At stage 3, *GmASH* expression forms a semicircle around the central region of the hemisegments (arrow). The former expression pattern of the anterior segments is now visible in leg

segment 3 (arrow). (C) *GmASH* expression has extended posteriorly to leg segment 5. The arrow points to the transient expression of *GmASH* in the invaginating cell groups. (D) After formation of all invagination sites, *GmASH* is still expressed in about half of them. In addition, the gene is expressed in the precursors of the peripheral nervous system (arrows). ant, antennal segment; l1 to l7, leg segments 1 to 7; md, mandibular segment; mx, maxillar segment; pmd, premandibular segment; pmx, premaxillar segment. Scale bar: 120 µm in A-D.
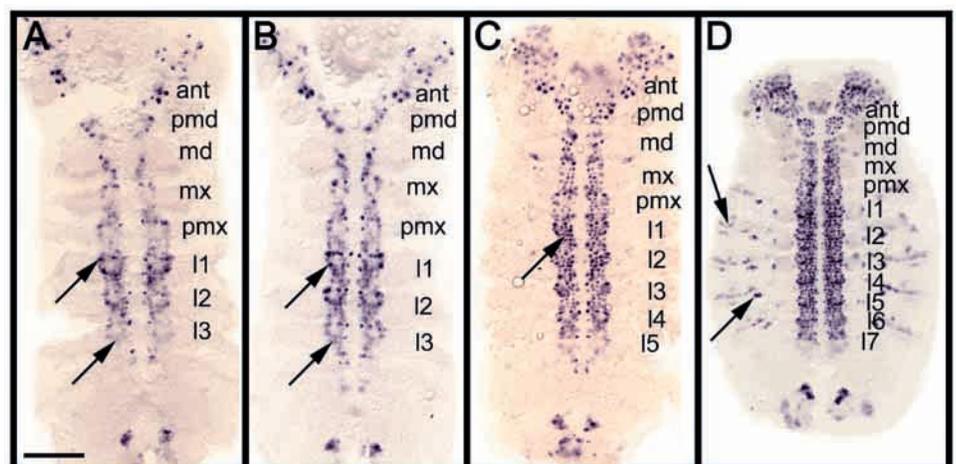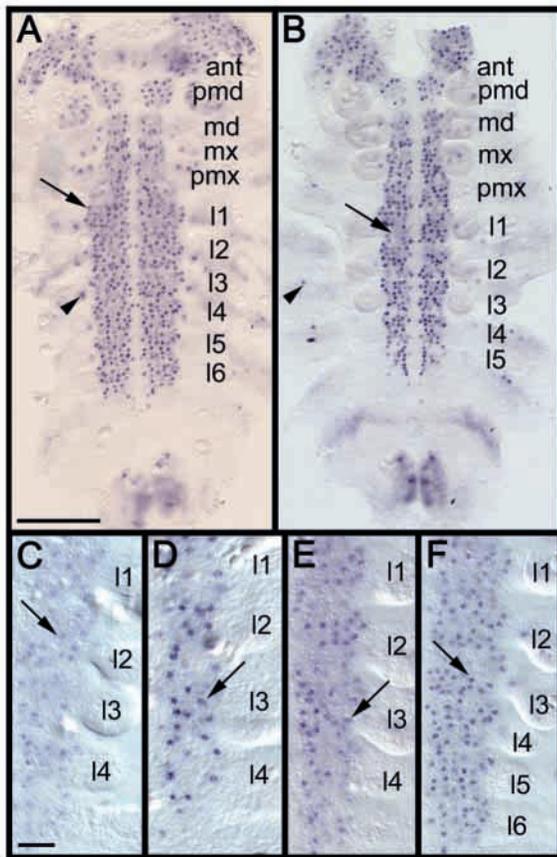
Fig. 9. (A-F) Expression pattern of *GmDelta*. Flat preparations of whole embryos (A,B) and leg segments (C-F) stained for a DIG-labelled *GmDelta* probe. (A,B) *GmDelta* transcripts can be detected at low levels in all ventral neuroectodermal cells, but they accumulate at higher levels in the invaginating cell groups. In addition, the gene is expressed in groups of cells in the limb buds and dorsal to the limb buds (arrowheads). These regions coincide with the generation sites of the peripheral nervous system. (C) Accumulation of higher levels of *GmDelta* transcripts is first visible during formation of the first invagination sites at stage 2 (arrow). (D-F) High levels of *GmDelta* expression correlate with the formation of invagination sites throughout neurogenesis (arrows). The expression is rapidly downregulated during the process of invagination, although the low uniform expression in all neuroectodermal cells is maintained. l1 to l6, leg segments 1 to 6. Scale bars: 120 μm in A,B; 50 μm in C-F.

Fig. 10. (A-F) Expression pattern of *GmNotch*. Flat preparations of whole embryos (A,B) and leg segments (C-F) stained for a DIG-labelled *GmNotch* probe. (A,B) At stage 4 *GmNotch* is expressed in all neuroectodermal cells (arrows) at heterogeneous levels. (C) At stage 1 *GmNotch* is expressed in segmentally repeated stripes, but shows a stronger expression in the ventral neuroectoderm (arrow). (D) During the first wave of neural precursor formation, *GmNotch* is expressed uniformly in the head segments and the first three leg segments (arrow). (E) The uniform expression resolves into a heterogeneous expression pattern before formation of the next wave of invagination sites. The arrowhead points to a region of low *GmNotch* expression, a higher expression is visible in the adjacent region (arrow). (F) *GmNotch* expression has extended posteriorly and still shows a heterogeneous expression pattern in the neuroectoderm. The expression in the limb buds probably corresponds to the formation of mesodermal tissue (arrowhead). ant, antennal segment; gz, growth zone; l1 to l5, leg segments 11 to 15; md, mandibular segment; mx, maxillar segment; pmd, premandibular segment; pmx, premaxillar segment. Scale bars: 120 μm in A,B; 50 μm in C-F.

heterogeneous expression during formation of the remaining invagination sites.

In summary, the data show that homologues of the *Drosophila Notch* and *Delta* genes are expressed in the ventral neuroectoderm during neurogenesis in a spatiotemporal pattern, suggesting that these genes are involved in the recruitment of neural precursors.

No decision between epidermal and neural fate

The cells in the ventral neuroectoderm of *Drosophila* have a choice between an epidermal and a neural fate. It has been shown recently, that this decision does not take place in the neurogenic region of the spider. Rather, all cells of the ventral neuroectoderm enter the neural pathway (Stollewerk, 2002).
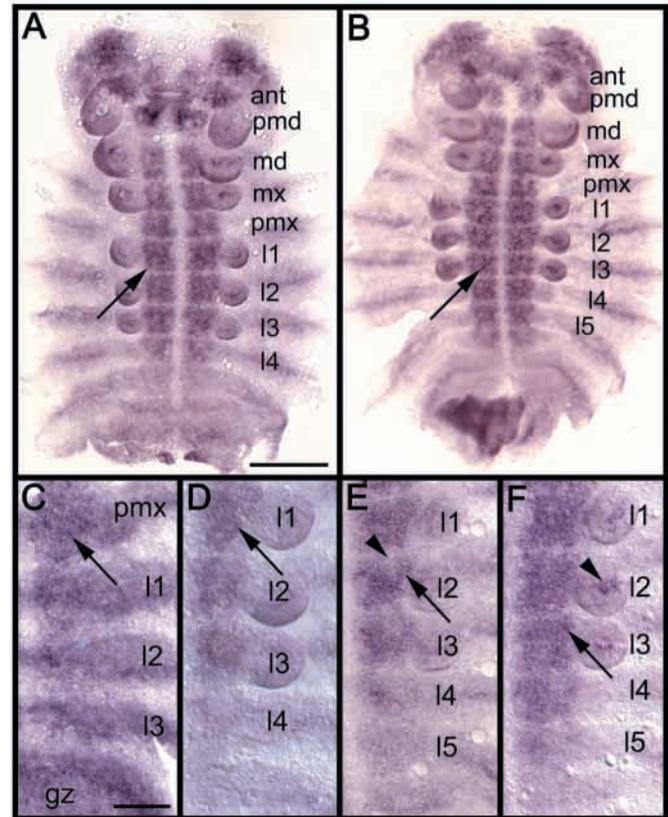
Analyses of transverse and horizontal sections of the ventral neuroectoderm of *Glomeris* embryos revealed that the invaginating cell groups detach from the apical surface at stage 6. At this stage a medial thickening forms in each hemineuromere (Fig. 11C). Subsequently, the neuroectoderm thickens at the lateral border adjacent to the limb buds (Fig. 11D) and the whole ventral neuromere sinks into the embryo while the epidermis overgrows the ventral nerve cord (Fig. 11A,D). At this time, a ladder-like axonal scaffold is already visible on the basal side (Fig. 11B), suggesting that there is no decision between epidermal and neural fate during the formation of neural precursors in the ventral neuroectoderm of *Glomeris*, as is the situation in the spider.

Fig. 11. (A-D) The epidermis overgrows the ventral nerve cord after formation of the neuropil. Flat preparations (A,B) and transverse semi-thin sections of the ventral nerve cords at stage 6. (A) Apical optical section of the ventral nerve cord of an embryo stained with phalloidin-rhodamine. The ventral neuromeres sink into the embryo (asterisk) and the epidermis overgrows the nerve cord (arrow). (B) Basal optical section of the same region shown in A. A ladder-like neuropil has been formed by the invaginated cells (arrow). (C) Transverse section of the hemineuromere of leg segment 1 at early stage 6. At this stage a medial thickening forms (arrowhead). The asterisk indicates the midline. (D) At late stage 6 an additional thickening has formed at the lateral border of the hemineuromere and the central part sinks into the embryo. The asterisk indicates the midline. l1 to l3, leg segments 1 to 3. Scale bars: 10 μm.
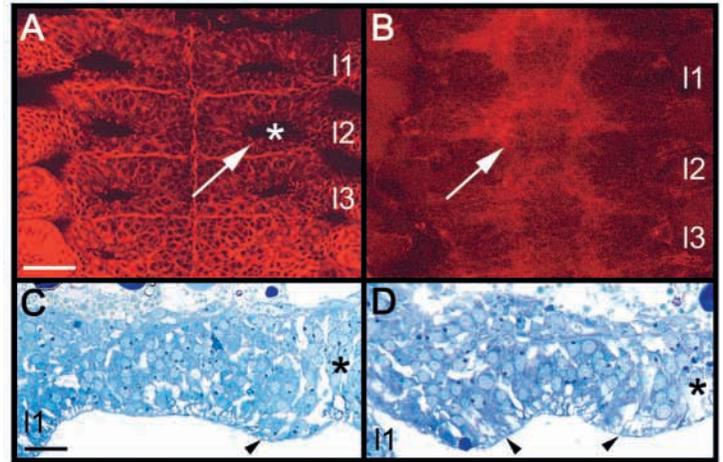
DISCUSSION

The pattern of invagination sites in *Glomeris* is strikingly similar to the spider

Our results show that, as in the spider, groups of cells invaginate from the ventral neuroectoderm of *Glomeris*. Number and arrangement of the invagination sites are strikingly similar to the spider pattern. In both the spider and *Glomeris*, there are about 30 invaginating cell groups arranged in a regular pattern of seven rows consisting of four to five invagination sites each. In addition, in both species the invaginating cell groups are generated in four waves. In contrast, in insects approx. 25 neuroblasts are generated per hemisegment that delaminate as individual cells from the ventral neuroectoderm in five waves. The first two populations of neuroblasts are arranged in three longitudinal columns and four rows per hemisegment. This regular pattern is lost after delamination of the next population of neuroblasts, because earlier born neuroblasts are shifted into a more basal position (Goodman and Doe, 1993). In summary these data show that the pattern of neural precursors and their mode of generation in *Glomeris* are more similar to those in the spider than in the insects.

However, there are some special features in the millipede that are different from spider neurogenesis. After formation of the first invagination sites, the ventral neuroectoderm forms a multi-layered structure of small cells, while in the spider there is only one single cell layer. The reason for this morphological difference is that because of limited space in the ventral neuroectoderm the invagination sites are located closer together and come to lie over and above each other. In addition, the invagination sites in *Glomeris* consist of up to 11 cells as compared to a maximum of eight in the spider and they do not all occupy a basal position. The invaginating cells do not all have the typical bottle-like shape as in the spider, so that their cell processes cover larger apical areas, and the dots of high phalloidin staining appear bigger in the millipede.

Furthermore, although the pattern of the invagination sites is very similar in the spider and *Glomeris*, the relative timing of generation of individual invagination sites is different. While in the spider the first invagination sites arise in the most anterior lateral region of the hemisegments, the first invaginating cell groups of the millipede are visible in the middle of the hemisegment. The next wave of invagination sites in the spider generates invaginating cell groups in coherent medial and posterior regions abutting the former generation sites. In contrast, in *Glomeris* newly formed invagination sites are distributed all over the hemisegment. Furthermore, the two most lateral anterior invagination sites that occupy strikingly similar positions in the spider and the millipede (see Fig. 1A,B) are generated during the first wave of invaginations in the spider, while they are not visible until the third wave of neural precursor formation in *Glomeris*.

However, the generation of neural precursors at stereotyped positions seems to be an ancient feature that has been maintained throughout the evolution of arthropods. Future analysis will show if the cells of an individual invagination site give rise to an invariant pattern of neurons in spiders and millipedes similar to the progeny of an identified neuroblast in insects and crustaceans.

Generation of neural precursors is associated with cell divisions in *Glomeris*

Studies of neurogenesis in different representatives of all myriapod groups have failed to reveal stem cell-like cells with the characteristics of insect or crustacean neuroblasts (Heymons, 1901; Tiegs, 1940; Tiegs, 1947; Dohle, 1964; Whitington et al., 1991). It is assumed that neurons are produced by a generalized proliferation of the ventral neuroectoderm. However, Knoll (Knoll, 1974) proposed that neuroblasts are present in the apical layer of the centipede *Scutigera coleoptrata* generating vertical columns of neurons; a mode of neural precursor formation that would be very similar to the crustacean pattern. Analysis of neurogenesis in another centipede, *Ethmostigmus rubripes*, led Whitington and co-workers (Whitington et al., 1991) to the assumption that neural precursors with the characteristics of insect neuroblasts are absent in this species. They could not detect sites of concentrated mitotic activity or dividing cells that are significantly larger than the surrounding cells. Similar results have been obtained for the spider: scattered mitotic cells are distributed over the neuroectoderm that do not prefigure regions where neural precursors form (Stollewerk et al., 2001). However, our analysis of the mitotic pattern in the ventral

neuroectoderm of *Glomeris* revealed that dividing cells are associated with invaginating neural precursors. Furthermore, groups of dividing cells seem to prefigure the regions where invagination sites arise. In contrast to the results from *Ethmostigmus* the dividing cells are significantly larger in size than the surrounding cells in the millipede. Therefore, we assume that stem cell-like cells are present in the apical layer of the ventral neuroectoderm in *Glomeris,* although this has to be confirmed by single cell labelling and BrdU injections. Since the dividing cell groups are located in the apical cell layer and are present before formation of the invagination sites, they are different from insect and crustacean neuroblasts. In *Drosophila* the neuroblasts do not divide until they delaminate from the outer layer. In contrast, the crustacean neuroblasts do not delaminate but remain in the apical layer, dividing parallel to the surface, so that the progenies are pushed to the basal side (Dohle and Scholtz, 1988; Scholtz, 1990; Scholtz, 1992).

The millipede pattern of neural precursor formation is intermediate when compared between chelicerates and insects. While in the spider neuroectodermal cells seem to divide randomly and are recruited for the neural fate because of their positions in the hemisegment, the presence of neural stem cells in the millipede links cell proliferation and generation of neural precursors in the apical cell layer. The necessity to single out epidermal and neural precursor cells from the ventral neuroectoderm in insects and crustaceans has led to a separation of the generation sites: epidermal cells are produced in the apical layer, while neural cells are generated on the basal side. Furthermore, the fact that neuroblasts are missing in almost all lower crustaceans analysed and that their mode of neurogenesis seems to be similar to that of myriapods, i.e. a separation of the ganglia into the interior (Anderson, 1973) indicates that an entirely neurogenic ventral neuroectoderm may be the ancestral state.

All cells of the neurogenic region enter the neural pathway in *Glomeris*

It is known that after completion of ventral flexure, the middle part of each hemisegment sinks into the embryo forming a groove (Dohle, 1964). During the course of neurogenesis this region is gradually incorporated into the embryo while epidermal cells overgrow the ventral nerve cord. We show here that this process does not take place until the final differentiation of the invaginated neural precursors, since a neuropil is already visible on the basal side, when the neuromeres sink into the embryo. This means that as in the spider, and in contrast to the situation in the insects, there is no decision between epidermal and neural fate in the central neurogenic region of the millipede.

Proneural and neurogenic genes in *Glomeris*

As in the spider and also in the insects, the *Glomeris achaete-scute* homologue is expressed before formation of neural precursors in the ventral neuroectoderm. Like the spider *CsASH1* gene, *GmASH* is expressed in patches of cells in the neuroectoderm and becomes restricted to the invaginating cell groups, while in insects proneural gene expression is reduced to one cell of the proneural cluster. After each wave of neural precursor formation *GmASH* is re-expressed in the regions where invagination sites form, indicating that the gene is

necessary for the formation of all neural precursors. However, this has to be confirmed by functional analysis.

During formation of neural precursors in *Drosophila*, the neurogenic genes *Notch* and *Delta* appear to be uniformly expressed in the neuroectoderm (Baker, 2000). Although it is assumed that within a proneural cluster the cell expressing the highest amounts of *Delta* is selected for the neural fate, no variation in *Delta* expression has yet been observed in the ventral neuroectoderm of fly embryos. In contrast, the expression patterns of the spider *Delta* genes can be correlated to the formation of neural precursors. While *CsDelta1* is exclusively expressed in neural precursors, *CsDelta2* transcripts are distributed uniformly throughout the neuroectoderm and accumulate in nascent neurons. The only *Delta* gene we have found in *Glomeris* is expressed similarly to the spider *CsDelta2* gene: at low levels in almost all neuroectodermal cells and at higher levels in the invaginating cell groups. Furthermore, although *Glomeris Notch* is initially expressed uniformly in the neuroectoderm, it resolves into a heterogeneous expression during the first wave of neural precursor formation similar to the spider *CsNotch* transcripts.

To summarize, our data support the hypothesis that myriapods are closer to chelicerates than to insects. The spider and the millipede share several features that cannot be found in equivalent form in the insects: in both the spider and the millipede, about 30 groups of neural precursors invaginate from the neuroectoderm in a strikingly similar pattern. Furthermore, in contrast to the insects, there is no decision between epidermal and neural fate in the ventral neuroectoderm of both species analysed. The sequence data also suggest a closer relationship of the millipede to the spider than to the insects. However, to confirm a sister group relationship of these arthropod groups, more morphological data from different representatives of myriapods, chelicerates and outgroups will be necessary.

REFERENCES

Abzhanov, A. and Kaufman, T. C. (2000). Crustacean (malacostracan) *Hox* genes and the evolution of the arthropod trunk. *Development* **127**, 2239-2249.

Abzhanov, A. and Kaufman, T. C. (1999). Homeotic genes and the arthropod head: Expression patterns of the *labial*, *proboscipedia*, and *Deformed* genes in crustaceans and insects. *Proc. Natl. Acad. Sci USA* **96**, 10224-10229.

Abzhanov, A., Popadic, A. and Kaufman, T. C. (1999). Chelicerate *Hox* genes and the homology of arthropod segments. *Evol. Dev.* **2**, 77-89.

Akam, M., Dawson, I. and Tear, G. (1988). Homeotic genes and the control of segment diversity. *Development* **104 Supplement**, 123-133.

Anderson, D. (1973). *Embryology and Phylogeny in Annelids and Arthropods*. Pergamon Press, Oxford.

Baker, N. E. (2000). Notch signalling in the nervous system. Pieces still missing from the puzzle. *BioEssays* **22**, 264-273.

Bierkamp, C. and Campos-Ortega, J. A. (1993). A zebrafish homologue of the Drosophila neurogenic gene *Notch*. *Mech. Dev.* **43**, 87-100.

Boore, J. L., Collins, T. M., Stanton, D., Daehler, L. L. and Brown, W. M.

(1995). Deducing the pattern of arthropod phylogeny from mitochondrial gene rearrangements. *Nature* **376**, 163-165.

Damen, W. G. M., Hausdorf, M., Seyfarth, E.-A. and Tautz, D. (1998). A conserved mode of head segmentation in arthropods revealed by the expression pattern of *Hox* genes in a spider. *Proc. Natl. Acad. Sci. USA* **95**, 10665-10670.

Damen, W. G. M. and Tautz, D. (1998). A *Hox* class 3 orthologue from the spider *Cupiennius salei* is expressed in a *Hox*-gene-like fashion. *Dev. Genes Evol.* **208**, 586-590.

Damen W. G. M., Weller, M. and Tautz, D. (2000). Expression patterns of *hairy*, *even-skipped*, and *runt* in the spider *Cupiennius salei* imply that these genes were segmentation genes in a basal arthropod. *Proc. Natl. Acad. Sci USA* **97**, 4515-4519.

Dohle, W. (1964). Die Embryonalentwicklung von *Glomeris marginata* (Villers) im Vergleich zur Entwicklung anderer Diplopoden. *Zool. Jahrb. Anat.* **81**, 241-310.

Dohle, W. (1997). Myriapod-insect relationships as opposed to an insect-crustacean sister group relationship. In: *Arthropod Relationships* (ed. R. A. Fortey und R. H. Thomas), pp. 305-316, London, Weinheim, New York, Tokyo, Melbourne, Madras: Chapman & Hall.

Dohle, W. (2001). Are insects terrestrial crustaceans? A discussion of some new facts and arguments and the proposal of the proper name 'Tetraconata' for the monophyletic unit Crustacea plus Hexapoda. *Annales de la Societe Entomologique de France* **37(1-2)**, 85-103.

Dohle, W. and Scholtz, G. (1988). Clonal analysis of the crustacean segment: the disarcordance between genealogical and segmental borders. *Development* **104 Supplement**, 147-160.

Friedrich, M. and Tautz, D. (1995). Ribosomal DNA phylogeny of the major extant arthropod classes and the evolution of myriapods. *Nature* **376**, 165-167.

Harzsch, S. and Dawirs, R. R. (1996). Neurogenesis in the developing crab brain: postembryonic generation of neurons persist beyond metamorphosis. *J. Neurobiol.* **29**, 384-398.

Heymons, R. (1901). Die Entwicklungsgeschichte der Scolopender. *Zoologica* **13**, 1-224.

Hwang, U. W., Friedrich, M., Tautz, D., Park, C. J. and Kim, W. (2001). Mitochondrial protein phylogeny joins myriapods with chelicerates. *Nature* **413**, 154-157.

Knoll, H. J. (1974). Untersuchungen zur Entwicklungsgeschichte von *Scutigera coleoptrata* L. (Chilopoda). *Zool. Jb. Anat.* **92**, 47-132.

Patel, N. H., Martin-Blanco, E., Coleman, K. G., Poole, S. J., Ellis, M. C., Kornberg, T. B. and Goodman, C. S. (1989a). Expression of *engrailed* proteins in arthropods, annelids, and chordates. *Cell* **58**, 955-968.

Patel, N. H., Kornberg, T. B. and Goodman, C. S. (1989b). Expression of *engrailed* during segmentation in grasshopper and crayfish. *Development* **107**, 201-212.

Scholtz, G. (1990). The formation, differentiation and segmentation of the post-naupliar germ band of the amphipod *Gammarus pulex* L. (Crustacea, Malacostraca, Peracarida). *Proc. Roy. Soc. London B* **239**, 163-211.

Scholtz, G. (1992). Cell lineage studies in the crayfish *Cherax destructor* (Crustacea, Decapoda): germ band formation, segmentation and early neurogenesis. *Roux's Arch. Dev. Biol.* **202**, 36-48.

Stollewerk, A., Klämbt, C. and Cantera, R. (1996). Electron microscopic analysis of midline glial cell development during embryogenesis and larval development using ß-galactosidase expression as endogenous marker. *Microsc. Res. Tech.* **35**, 294-306.

Stollewerk, A. (2000). Changes in cell shape in the ventral neuroectoderm of *Drosophila melanogaster* depend on the activity of the *achaete-scute* complex genes. *Dev. Genes Evol.* **210**, 190-199.

Stollewerk, A., Weller, M. and Tautz, D. (2001). Neurogenesis in the spider *Cupiennius salei*. *Development* **128**, 2673-2688.

Stollewerk, A. (2002). Recruitment of cell groups through Delta/Notch signalling during spider neurogenesis. *Development* **129**, 5339-5348.

Telford, M. J. and Thomas, R. H. (1998). Expression of homeobox genes shows chelicerate arthropods retain their deuterocerebral segment. *Proc. Natl. Acad. Sci. USA* **95**, 10671-10675.

Tiegs, O. W. (1940). The embryology and affinities of the Symphyla based on the study of *Hanseniella agilis*. *Q. J. Microsc. Sci.* **82**, 1-225.

Tiegs, O. W. (1947). The development and affinities of the Pauropoda based on the study of *Pauropus sylvaticus*. *Q. J. Microsc. Sci.* **88**, 165-267/175-336.

Whitington, P. M., Meier, T. and King, P. (1991). Segmentation, neurogenesis and formation of early axonal pathways in the centipede, *Ethmostigmus rubrides* (Brandt). *Roux's Arch. Dev. Biol.* **199**, 349-363.